ANNUAL REPORT FOR DE-FG07-02ER63494
ENVIRONMENTAL MANAGEMENT SCIENCE PROGRAM PROJECT NUMBER 87016
CO-PRECIPITATION OF TRACE METALS IN GROUNDWATER AND VADOSE ZONE CALCITE: *IN SITU* CONTAINMENT AND STABILIZATION OF STRONTIUM-90 AND OTHER DIVALENT METALS AND RADIONUCLIDES AT ARID WESTERN DOE SITES

Investigators:

Principal Investigator

F. Grant Ferris
University of Toronto
Toronto, Ontario
Canada M5S 3B1
(416) 978-0526
ferris@geology.utotonto.ca

Co-Principal Investigators

Yoshiko Fujita
Idaho National Engineering and
Environmental Laboratory
Idaho Falls, ID 83415
(208) 526-1242
fujiy@inel.gov

Robert W. Smith
University of Idaho-Idaho Falls
Idaho Falls, ID 83402
(208) 282-7954
smithbob@uidaho.edu

Other Senior Contributors:

Donna M. Cosgrove
University of Idaho-Idaho Falls
Idaho Falls, ID 83402
(208) 282-7914
cosgrove@if.uidaho.edu

F. "Rick" S. Colwell
Idaho National Engineering and
Environmental Laboratory
Idaho Falls, ID 83415
(208) 526-0097
fxc@inel.gov

Report prepared by Dr. Andrew Mitchell. Post-Doctoral Research Fellow. Department of Geology, University of Toronto, 22 Russell Street, Toronto. Ontario. Canada. M5S 3B1.(416) 978-0549. andy@geology.utotonto.ca

1. INTRODUCTION

Radionuclide and metal contaminants are present in the vadose zone and groundwater throughout the U.S. Department of Energy (DOE) weapons complex. *In situ* containment and stabilization of these contaminants in vadose zones or groundwater is a cost-effective treatment strategy. Our facilitated approach relies upon the hydrolysis of introduced urea to cause the acceleration of calcium carbonate precipitation (and trace metal co-precipitation) by increasing groundwater pH and alkalinity (Fujita *et al*., 2000; Warren *et al*., 2001). Subsurface urea hydrolysis is catalyzed by the urease enzyme, which may be either introduced with the urea or produced *in situ* by ubiquitous subsurface urea hydrolyzing microorganisms. Because the precipitation processes are irreversible and many western aquifers are saturated with respect to calcite, the co-precipitated metals and radionuclides will be effectively removed from groundwater. The rate at which trace metals are incorporated into calcite is a function of calcite precipitation kinetics, adsorption interactions between the calcite surface and the trace metal in solution (Zachara *et al*., 1991), solid solution properties of the trace metal in calcite (Tesoriero and Pankow, 1996), and also the surfaces upon which the calcite is precipitating. A fundamental understanding of the coupling of calcite precipitation and trace metal partitioning, and how this occurs in aquifers and vadose environments is lacking. This report summarizes work undertaken during the second year of this project.

2. RESEARCH OBJECTIVES

The objectives of this research are to: a) elucidate the mechanisms and rates for the release of sorbed trace metals and their subsequent sequestration by co-precipitation in calcite induced by urea hydrolysis, b) evaluate at the field scale the influence of microbial calcite precipitation on the partitioning and retention of strontium and other naturally occurring divalent metals in groundwater, and c) to identify specific microbial community characteristics that signify subsurface geochemical conditions conducive to calcite precipitation.

These objectives are being accomplished by conducting integrated field and laboratory research. This report summaries progress in the laboratory component of the work in the second year of this project. Specifically this includes experiments investigating (i) controls on the co-precipitation of Sr, and (ii) mechanisms of calcite nucleation and crystal growth.

3. RESEARCH PROGRESS AND IMPLICATIONS

3.1. Controls on the co-precipitation of Sr (Mitchell *et al.*, in review)

3.1.1. Materials and Methods

A suite of experiments investigating the co-precipitation of Sr in calcite precipitated in response to the hydrolysis of urea by *Bacillus pasteurii* ATCC 11859 have been completed under conditions that simulate *in-situ* conditions. This has been undertaken using an artificial groundwater (AGW) based upon the aqueous chemistry of the Snake River Plain Aquifer (SRPA) (Knobel *et al.*, 1992) in the vicinity of the Idaho National Engineering and Environmental Laboratory.

The methods used here are a modification of those used by Ferris *et al.* (2004). Experiments were performed in microcosms inoculated with *B. pasteurii* and containing the AGW. The AGW contained Sr at 0.1 mM, to mimic the contaminant radionuclide ^{90}Sr. Microcosms also contained 6.0 mM urea (for experiments ran at 20 ^{o}C) and 25 mM urea (for experiments ran at 10 and 15 ^{o}C). Throughout the experiment the experimental solutions were monitored for ammonium, dissolved calcium and strontium content and pH. Mineral precipitates that formed during incubation were identified by powder X-ray diffraction (XRD). Experimental data was used for integrated equations for urea hydrolysis, calcite saturation state and dissolved calcium concentrations, using unconstrained nonlinear regression and a quasi-Newton optimization routine for parameter estimation (STATISTICA v 5.0).

The efficiency of Sr co-precipitation in calcite was assessed using phenomenological partition coefficients (Curti, 1999). The partition coefficient for Sr in calcite precipitates was calculated as follows, as originally defined by Doerner and Hoskins (1925):

$$D_{Me} = \frac{\{Me\}_{surface}}{[Me]} \Big/ \frac{\{Ca\}_{surface}}{[Ca]} \qquad [1]$$

where D_{Me} is the heterogeneous partition coefficient for the incorporation of the trace metal, Me, in calcite, $\{Me\}_{surface}$ and $\{Ca\}_{surface}$ are the mole fractions of the co-precipitated trace element and Ca respectively at the surface of calcite, and [Me] and [Ca] are the concentration of the trace metal and Ca in solution. The definition of terms *heterogeneous* partition coefficient, and *surface* indicates the precipitated solid is not in a state of internal equilibrium, and the solution is in equilibrium only with the uppermost monolayer of the precipitated solid. This relationship is true of closed natural and experimental systems where the composition of the solution varies over time as co-precipitation proceeds, and thus the distribution of the trace element in calcite is not uniform, but rather will exhibit zoned crystals where the concentration of the trace element will vary between the core to the surface. Precipitates with a heterogeneous composition will generally result from variations of the [Ca]/[Me] during the experiment (Curti, 1999).

Because of the complexities of determining the surface composition of precipitated solids, in this study we determine the D_{Me} using the *total* mass of Ca and Sr in the precipitated solid, and the solution composition at the sampling time (e.g. Tesoriero and Pankow, 1996). This generates an instantaneous heterogeneous partition coefficient for the experimental system at the sampling time. The *total* mass of Ca in the precipitated solid ($[Ca]_{solid}$) was determined at individual sampling times from simple mass balance according to;

$$[Ca]_{solid} = [Ca]_0 - [Ca]_t \qquad [4]$$

where '0' denotes the initial concentrations and 't' denotes the sampling time. This was calculated similarly for Sr, and allowed the mole fractions of {Ca} and {Sr} in the calcite precipitate to be determined.

3.1.2. Results and Discussion

During the experiments ammonium concentration from bacterial urea hydrolysis increased asymptotically, and derived rate constants (k_{urea}) that were between 13 and 10 times greater at 20°C, than at 15 and 10°C (Table 1). Calcite precipitation was initiated after similar amounts of urea had been hydrolyzed (~ 4.0 mmoles L^{-1}) (Figure 1) and a similar critical saturation state (mean $S_{critical}$ = 53, variation = 20 %) had been reached, independent of temperature and Sr treatment (Table 1). Because of the positive relationship between urea hydrolysis rate and temperature, precipitation began by the end of day 1 at 20°C, and between days 1 and 2 at 15 and 10°C. The rate of calcite precipitation decreased during the experiments, but increased with, and was fundamentally controlled by calcite saturation state (*S)* (Figure 2). The presence of Sr slightly slowed calcite precipitation rates at equivalent values of *S*, which may reflect the screening of active nucleation and crystal growth sites by Sr (Figure 2).

Table 1. Summary of kinetic parameters for urea hydrolysis (k_{urea}), change in saturation state (k_S), calcite precipitation (k_P), apparent critical saturation (S_0), effective critical saturation (S_{crit}) in the AGW and AGW plus Sr experiments at different experimental temperatures.

Temperature °C	Mixture	k_{urea} (day^{-1})	k_s (day^{-1})	k_p ($\mu moles L^{-1} day^{-1}$)	S_{crit}	S_0
10	AGW	0.07	0.12585	0.203	49	50
10	AGW + Sr	0.07	0.09412	0.121	56	58
15	AGW	0.07	0.1368	0.243	45	49
15	AGW + Sr	0.07	0.14459	0.194	51	55
20	AGW	0.73	0.178	0.171	57	59
20	AGW + Sr	0.99	0.1794	0.183	57	61

Figure 1. Dissolved concentration of Ca^{2+} as a function of ammonium concentration in (a) the AGW experiment and (b) the AGW + Sr experiment.

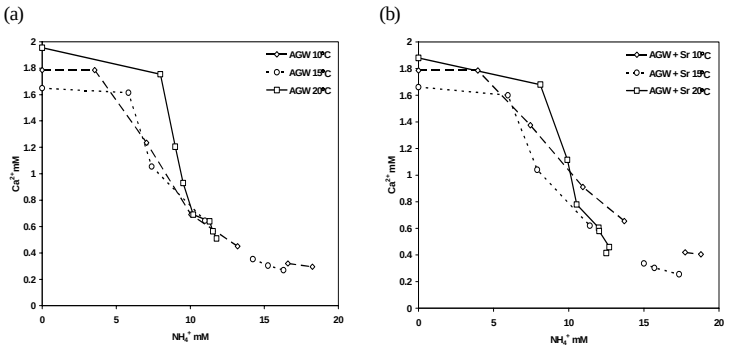

Figure 2. Calcite precipitation rate as a function of (a) time, and (b) calcite saturation state during the AGW and AGW + Sr experiments at 10, 15 and 20°C.

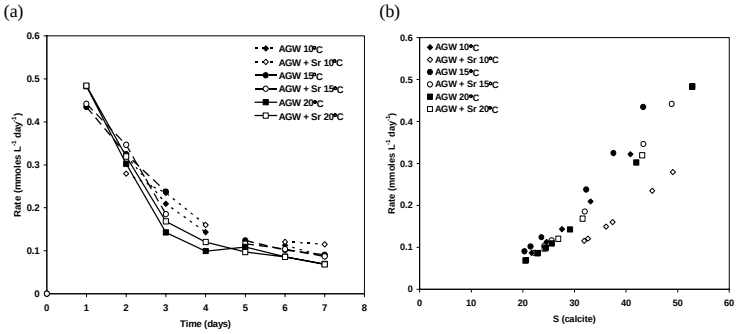

The co-precipitation of Sr was greater at higher calcite precipitation rates, and at equivalent precipitation rates at higher experimental temperatures, with respect to (i) the proportion of Sr in the aqueous system (Figure 3), (ii) the mass precipitated relative to Ca (Sr/Ca) and (iii) the mass precipitated relative to solution concentration (D_{Sr}: 20°C mean = 0.46; 15°C mean = 0.24; 10°C mean = 0.29) (Figure 4). This rate dependence is likely to reflect the large Sr ion, which cannot fully co-ordinate relative to ions smaller than Ca at equilibrium conditions, but is increasingly co-precipitated as all ions are indiscriminately incorporated at higher precipitation rates. The temperature dependence is likely to reflect the higher miscibility of ions in minerals at higher temperatures. Partition coefficients for Sr in calcite were more than an order of magnitude higher than reported in other studies, even if extrapolated to very low precipitation rates. High partition coefficients generated by the bacterial hydrolysis of urea are exceptionally promising for an engineered groundwater remediation strategy.

Figure 3. The percentage of total Sr in the AGW + Sr experimental system ($Sr_{[total]}$) in calcite precipitates as a function of (a) time, and (b) calcite precipitation rate at 10, 15 and 20°C.

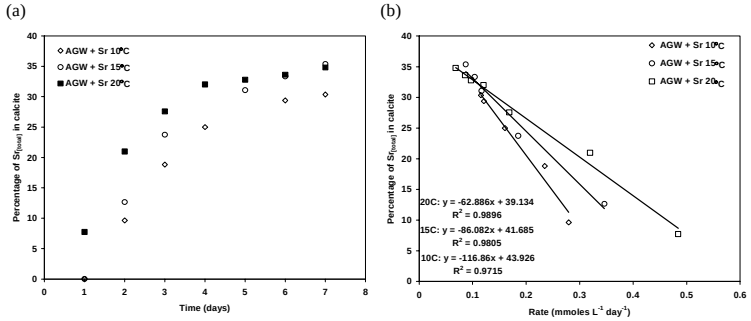

Figure 4. The co-precipitation of Sr in calcite precipitates induced by the hydrolysis of urea by *B. pasteurii* in the AGW + Sr experimental system as a function of precipitation rate; (a) Sr/Ca ratios and (b) Partition coefficients. Plate 1 (left). Example calcite precipitates, indicating calcite occurring on, or proximal to the bacteria (A and B), and examples of resulting crystal morphologies after some degree of crystal growth.

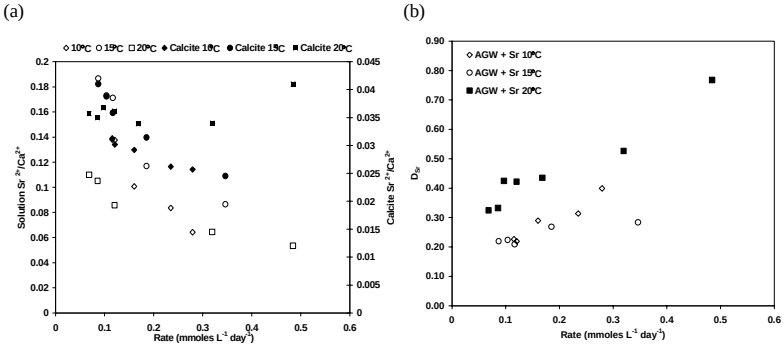

3.2. Mechanisms of nucleation and calcite crystal growth – evidence from crystal size distributions

3.2.1. Materials and Methods

Calcite precipitates from previous experiments demonstrate ureolytic bacteria buried within growing calcite crystals (Figure 5). However, the actual precipitation mechanisms and the physical effect of bacteria surfaces on these processes is unclear. A suite of experiments were performed in order to investigate the mechanisms of calcite precipitation by bacterial ureolysis utilizing calcite crystal size distributions (CSDs) (McCoy, 2001).

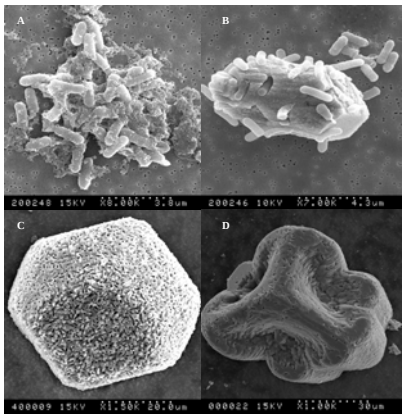

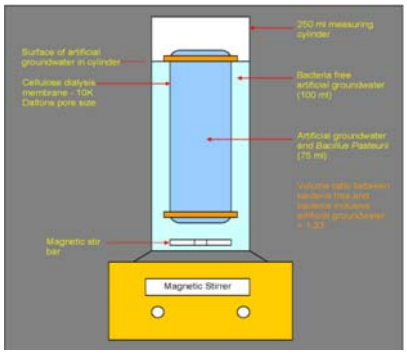

Duplicate experiments were performed at 15ºC over 7 days in microcosms containing AGW and 25 mM urea. Microcosms were inoculated with the ureolytic bacteria, *B. pasteurii*. In a separate set of microcosms, *B. pasteurii* and AGW was contained within a cellulose dialysis membrane with a 10 K Daltons pore size, which was submerged in an approximately equal volume of AGW. The dialysis membrane allowed solute to pass through but not bacteria. This resulted in a bacteria-inclusive and bacteria-free AGW solution (Figure 6). These microcosms were constantly mixed with a magnetic stir bar. Extracted calcite precipitates were analysed by scanning electron microscopy. Crystal measurements were undertaken on these images using ImageJ (v.1.31). CSDs were generated in STATISTICA v.5 using log-normal distribution fitting.

Figure 5 (Above left). Calcite precipitates generated by bacterial ureolysis. Figure 6 (Below left). Schematic diagram of dialysis experimental set up

3.2.2. Results and Discussion

Ammonium concentration generated by bacterial ureolysis increased during the duration of the experiments, resulting in the precipitation of calcite at supersaturation, and a decrease in dissolved Ca^{2+} to almost zero by day 4 (Figure 7). In the dialysis experiments, identical changes in solution chemistry were exhibited in the bacteria-free and bacteria-inclusive AGW solution, but calcite formation was observed earlier in the bacteria-free AGW.

Lognormal distribution fitting provided an excellent fit of the calcite crystal size data (Table 2). Calcite CSDs generated from the mixed AGW and bacteria experiments exhibit an increase in peak (mode) and median of crystal size (CS) from days 1 to 4, whereas from days 4 to 6, the peak and median CS remained the same. The variance of CS decreased from days 1 to 2 but increased thereafter. These characteristics are demonstrated by a slight widening and general decreasing negative skew of the CSD over time, and a decreasing frequency of peak CS (Figure 8).

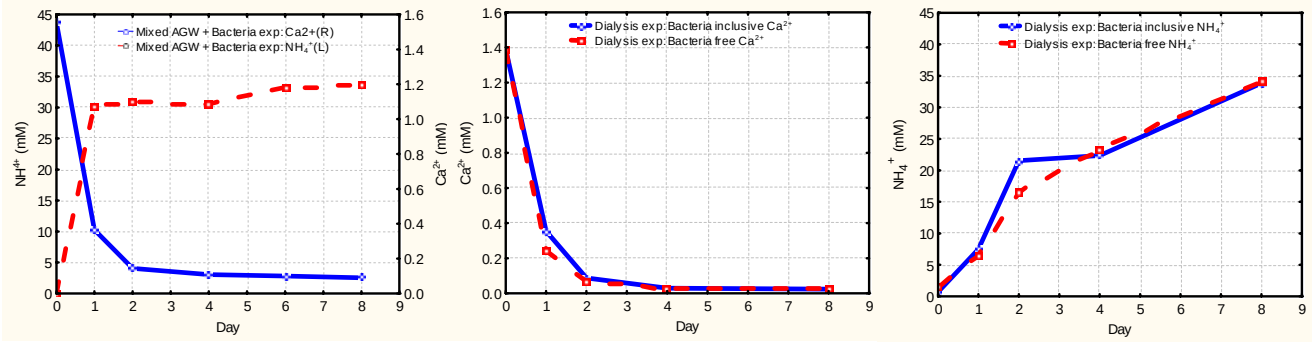

Figure 7. Solution chemistry in the mixed AGW and B. Past experiments, and dialysis experiments with bacteria-free and bacteria-inclusive AGW.

Table 2. Summary statistics of crystal size distributions from the experiments (Units = um).

Experiment	Day	Median (um)	Mode (um)	10th Percentile (um)	90th Percentile (um)	Variance (%)	Skewness	Kurtosis	r^2 of observed v expected CSD distribution fitting
Mixed AGW + B. Pasteurii	1	0.57	0.35	0.29	1.8	6.7	16	300	0.93
	2	0.63	Multiple	0.35	1.3	0.68	12	200	0.95
	4	0.8	0.49	0.44	1.8	3.1	17	350	0.96
	6	0.8	0.49	0.47	1.7	18	10	100	0.91
Dialysis experiments Separating AGW + B. Pasteurii									
Bacteria free AGW	1	2.2	1.8	1.2	3.7	1.5	2.0	6.9	0.97
Bacteria free AGW	7	4.1	Multiple	1.9	7.5	83	12	140	0.85
Bacteria inclusive AGW	1	2.2	1.5	0.9	8.5	56	5.4	38	0.87
Bacteria inclusive AGW	7	12	Multiple	3.7	17	26	0.16	0.31	0.34

In the dialysis experiments similar growth mechanisms were observed, where in both the bacteria-free and bacteria-inclusive AGW there is an increase in the peak, median, minimum, maximum and variance of crystal size over time (Figure 8). Significantly, the presence of *B. pasteurii* in the AGW increased the peak, median, mean and variance crystal size relative to the bacteria-free AGW over time (Table 2) in response to the same changes in solution chemistry (Figure 7).

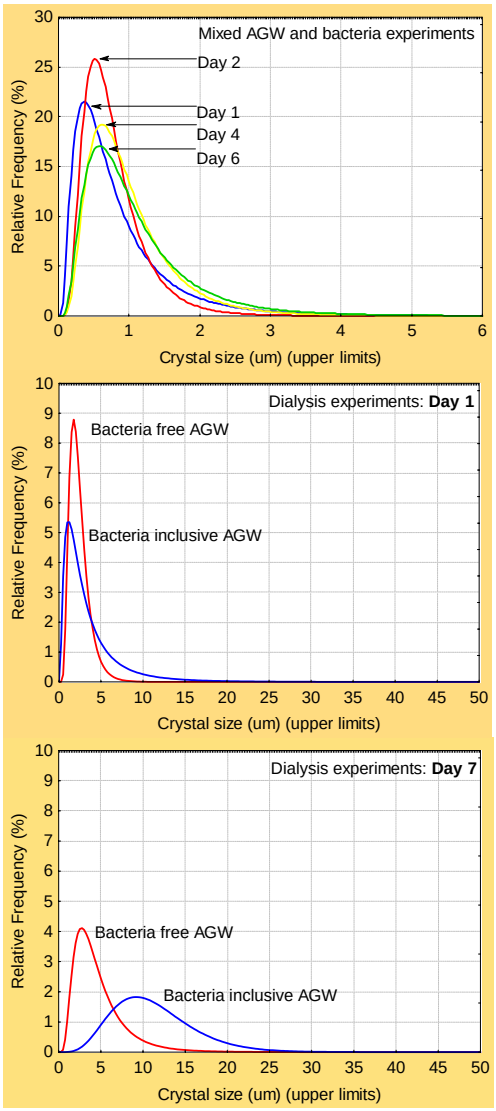

The mechanism of calcite precipitation in response to bacterial ureolysis appears to follow the model for crystal growth in unsteady-state batch systems (McCoy, 2001) where nucleation at the point of supersaturation is followed by crystal growth. In the mixed AGW and bacteria experiments, growth appears surface-controlled up to day 4, but the exhaustion of dissolved Ca^{2+} by day 4, and the approximately equal CSD on days 4 and 6 suggests a steady-state CSD has been attained by supply-limited growth. No reduction in the variance of CSDs and the frequency of smaller CSs between days 4 and 6 suggests crystal ripening is not occurring. Nucleation of calcite by bacterial ureolysis is probably by a combination of homogeneous nucleation in the bulk solution and heterogeneous nucleation on nascent crystals and on bacterial cell surfaces. Indeed, the difference in CSDs between the bacteria-inclusive and bacteria-free AGW indicates bacterial surfaces actively affect calcite precipitation processes. The apparent delay in calcite precipitation observed in the bacteria-inclusive relative to the bacteria-free AGW suggests *B. pasteurii* may actively inhibit calcite precipitation.

These preliminary data demonstrate the utility of CSDs for understanding mechanisms of biomineralization, and may be important for predicting and limiting the transport and dissolution of contaminated solids in groundwater systems. Anysis of these data is ongoing at present.

Figure 8. Crystal size distributions generated in the mixed AGW and B. Past experiments, and dialysis experiments with bacteria-free and bacteria-inclusive AGW.

4. RECENT AND PLANNED ACTIVITIES

The results thus far represent an idealised system that does not include aquifer minerals. The host mineral matrix may effect calcite precipitation by ureolytic bacteria in two ways. First, the mineral matrix provides abundant sites for two-dimensional heterogeneous nucleation and crystal growth, where the interfacial activation energy barrier for nucleation is decreased. Secondly, aquifer minerals comprise a large reservoir of exchangeable divalent cations that are likely to participate in the precipitation process. Therefore, recently, experiments have been performed to investigate the effect of host aquifer basalt on the precipitation process. Double strength AGW with Sr containment treatment was equilibrated with the basalt for two weeks in individual reaction vessels. The vessels were then inoculated with *B. pasteurii*. The solution chemistry was monitored and calcite crystals and samples of the basalt were taken for SEM analysis. This work is proceeding at the moment.

The next phase of experiments will investigate the temperature and kinetic dependence of the co-precipitation of other contaminants (Co, Cd, U, Zn), and the competition effects of such species in the precipitation process. Specifically we wish to determine the partition coefficient for these other species is related to the calcite precipitation rate. It is likely that ions smaller than Ca will exhibit is inverse relationship between the partition coefficient and precipitation rate, unlike the positive relationship exhibited by Sr (Mitchell *et al*., in review; Curti, 1999).

5. INFORMATION ACCESS

Publications arising from work completed so far:

Ferris, F.G., Phoenix, V., Fugita, Y and Smith, R.W. (2004) Kinetics of Calcite Precipitation Induced by Ureolytic Bacteria at 10°C to 20°C in Artificial Groundwater. Geochimica et Cosmochimica Acta. GCA 68(8), 1701-1722.

Mitchell, A.C., Mancini, A., Litwin, Y. and Ferris, F.G. (in review) The Co-Precipitation of Sr into Calcite Precipitates Induced by Bacterial Ureolysis in Artificial Groundwater – Temperature and Kinetic Dependence. GCA.

Conference presentations:

Andrew C. Mitchell and F. Grant Ferris. The Co-Precipitation of Sr into Calcite Induced by Bacterial Ureolysis in Artificial Groundwater – Temperature and Kinetic Dependence. Poster presentation. AGU 2003. San Francisco, December 2003.

Andrew C. Mitchell, Lisa Magalhaes, Andrew Mancini and F. Grant Ferris. Mechanisms of calcite precipitation by bacterial ureolysis – evidence from crystal size distributions. Poster presentation. Goldschmidt 2004. Processes in Geochemistry, Copenhagen, June 6th – 12th 2004.

References

Curti E. (1999) Co precipitation of radionuclides with calcite: estimation of partition coefficients based on a review of laboratory investigations and geochemical data. *Applied Geochemistry* **14**(4), 433-445.
Doerner, H.A and Hoskins W.M. (1925) Co-precipitation of radium and barium sulphates. *J. Am. Chem. Soc*. **47**, 662-675.
Fujita, Y., Ferris, F.G., Lawson, R.D., Colwell, F.S., and Smith, R.W. (2000) Calcium carbonate precipitation by ureolytic subsurface bacteria. *Geomicrobiol. J.* **17**, 305-318.
Knobel L. L., Bartholomay R.C., Cecil L.D., Tucker B.J., and Wegner S.J. (1992) Chemical constituents in the dissolved and suspended fractions of ground water from selected sites, Idaho National Engineering Laboratory and vicinity, Idaho, 1989. Idaho Falls, U. S. Geological Survey. Open-File Report 92-51.
McCoy, B.J. (2001) A New Population Model for Crystal Size Distributions: Reversible, Size-Dependent Growth and Dissolution. *Journal f Colloid and Interface Science* 240, 139-149.
Tesoriero, A.J. and Pankow, J.F. (1996) Solid Solution Partitioning of Sr2+, Ba2+, and Cd2+ to Calcite. *Geochim. Cosmochim. Acta* **60**, 1053-1063.

Warren L.A., Maurice P.A., Parmar N., and Ferris F.G. (2000) Microbially mediated calcium carbonate precipitation: implications for interpreting calcite precipitation and for solid phase capture of inorganic contaminants. *Geomicrobiol. J.* **18**, 93-115.
Zachara, J.M., Cowan, C.E., and Resch, C.T. (1991) Sorption of Divalent Metals on Calcite. *Geochim. Cosmochim. Acta* **55**, 1549-1562.